Available online at www.sciencedirect.com

ScienceDirect

Journal of Electroanalytical Chemistry 599 (2007) 203–208

Journal of Electroanalytical Chemistry

www.elsevier.com/locate/jelechem

Pore entrance effects on the electrical potential distribution in charged porous membranes and ion channels

Vladimir García-Morales, Javier Cervera [1], José A. Manzanares *

Departament de Termodinàmica, Universitat de València, C/Dr. Moliner 50, E-46100 Burjassot, Spain

Received 19 October 2005; received in revised form 22 December 2005; accepted 27 December 2005
Available online 3 February 2006

Dedicated to Professor David J. Schiffrin

Abstract

Models for the electrical potential distribution in the interfacial region between a fixed charge membrane and an electrolyte solution have traditionally employed the Donnan equilibrium formalism that assumes discontinuous changes in concentrations and electric potential. In the case of the charged capillary membrane model, we propose to check rigorously the validity of this approach by solving the linearized Poisson–Boltzmann equation for the diffuse electrical double layer at the membrane|solution interface. The comparison of the resulting axial distribution for the electric potential with the Donnan potential drop shows that the discontinuous approach is only valid for membrane thicknesses much greater than the Debye length of the problem.

Keywords: Charged capillary model; Membrane|solution interface; Poisson–Boltzmann equation; Ion channels

Models for porous charged membranes have usually considered the membrane as composed by an array of identical parallel capillary pores and have assumed the Donnan equilibrium discontinuous approach at the membrane|solution interface. The model has proved useful not only for synthetic filters but also for biological membranes. The membrane pores shows ionic selectivity because the electrical charges attached to the pore surface create an electrical double layer (EDL) that extends from the surface to the center of the pore. If the concentration of the mobile ions is low enough, the diffuse double layer theory can give a suitable description of the radial ionic distributions across the pore [1]. Therefore, the Gouy–Chapman approach for the EDL at the pore surface, together with the Nernst–Planck flux equation and the Navier–Stokes equation describing the solution flow through the charged capillary, have constituted the basis of most treatments for ion transport through charged capillary pores. This charged capillary model has been able to describe the coupling between the mass and electrical fluxes through charged membranes in many experimental situations [2].

However, the theory contains several compromising assumptions, some of which concern the spatial distribution of the electrical potential. In order to make negligible the pore entrance (or edge) effects, the pore length is invariably considered to be much larger than the Debye length. More importantly, at the membrane|solution interface the electric potential distribution is assumed to be discontinuous, as an straightforward extension of the classical one-dimensional Donnan formalism [1]. Thus, although considerable effort is devoted in the charged capillary model to the radial distribution of electric potential across the pore cross-section [2–5], this is not the case of the axial distribution of electric potential at the membrane boundaries, which should also be obtained from the solution of the Poisson–Boltzmann (PB) equation. Except for a few studies restricted to one-dimensional membrane systems,

---

* Corresponding author. Tel.: +34 96 354 4487; fax: +34 96 354 3385.
E-mail address: manzanar@uv.es (J.A. Manzanares).

[1] Present address: Departament de Ciencies Experimentals, Universitat Jaume I, Campus Riu Sec, 12080 Castelló de la Plana, Spain.

0022-0728/$ - see front matter © 2006 Elsevier B.V. All rights reserved.
doi:10.1016/j.jelechem.2005.12.025

where only the axial coordinate is considered [6–10], the relationship between the discontinuous (Donnan) formalism at the membrane|solution interface and that resulting from the PB equation has not been discussed in detail. This can be attributed to the difficulty of finding a solution of the PB equation in the interfacial region from the charge cylindrical pore but also in the external solutions. In this note, such a solution is described and used to obtain quantitative results for the difference between the actual potential drop in the interfacial region and the approximate result obtained from the discontinuous formalism. Thus, for instance, the expectation that the discontinuous formalism could be used for the charged capillary model in those cases where the membrane thickness is much greater than the Debye length characteristic of the EDL [10,11] can be rigorously checked. The results here presented on the axial structure of the EDL can be relevant not only for synthetic thick membranes [12] but also for the electrical properties of thin biological membranes and ion channels [1,13].

There are two well-known approximate solutions to the PB equation that correspond to the limiting cases of small and high values of the electric potential ϕ (when compared to the thermal potential RT/F, where F, R and T are the Faraday constant, the gas constant, and the thermodynamic temperature, respectively). An analytical solution to the linearized Poisson–Boltzmann (LPB) equation exists in the first case [2,14,15]. Although the range of validity of this solution is limited [2], it shows the essential trends of the problem [14,15] and will be used here for the sake of simplicity. More general solutions to the PB equation that make use of variational and numerical methods [3,4,16–18] can be found in the literature.

The equilibrium electrical potential distribution in the interfacial region between a 1:1 binary electrolyte solution of concentration c and a semi-infinite charged cylindrical pore of radius a is studied first (see Fig. 1a). The pore is considered to occupy region $x > 0$, where x is the position coordinate along the pore axis. A uniform surface charge density σ is smeared over the pore walls. This charge density is assumed to be small enough so that the low potential approximation $F|\phi|/RT \ll 1$ remains valid. This potential distribution must be obtained from the solution of the LPB equation in cylindrical coordinates

$$\frac{1}{r}\frac{\partial}{\partial r}\left(r\frac{\partial\phi}{\partial r}\right)+\frac{\partial^2\phi}{\partial x^2}=\kappa^2\phi \tag{1}$$

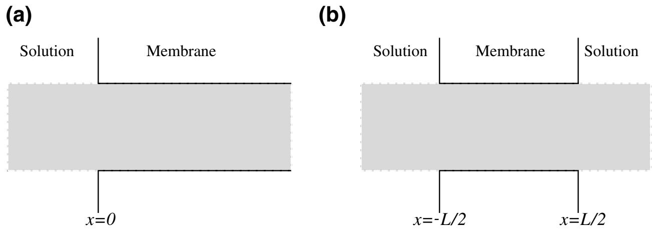

Fig. 1. Interfacial regions considered: (a) semi-infinite pore and external solution, (b) finite pore of length L and external solutions.

subject to the boundary conditions

$$\left.\frac{\partial\phi}{\partial r}\right|_{r=0}=0 \tag{2}$$

$$\left.\frac{\partial\phi}{\partial r}\right|_{r=a}=\frac{\sigma}{\varepsilon}H(x) \tag{3}$$

where $\kappa \equiv (2F^2c/\varepsilon RT)^{1/2}$ is the reciprocal Debye length, ε is the electrical permittivity of the solution filling the pore, and $H(x)$ is the step function (1 if $x > 0$ and 0 if $x < 0$).

It is well-known that the solution to Eq. (1) inside the pore far from the interface (i.e., when $\partial^2\phi/\partial x^2 = 0$) is [14,15]

$$\phi_\infty(r)=\lim_{x\to\infty}\phi(r,x)=\frac{\sigma}{\varepsilon\kappa}\frac{I_0(\kappa r)}{I_1(\kappa a)} \tag{4}$$

where I_0 and I_1 are the zeroth-order and first-order modified Bessel functions of first kind, respectively, and the origin of potentials ($\phi = 0$) has been established in the bulk solution ($x \to -\infty$).

The general solution to Eq. (1) can be obtained by the method of separation of variables [19] as

$$\phi(r,x)=\int_{-\infty}^{\infty}C_\lambda I_0(\kappa_\lambda r)\mathrm{e}^{\mathrm{i}\lambda\kappa x}\,\mathrm{d}\lambda \tag{5}$$

where $\kappa_\lambda \equiv \kappa\sqrt{1+\lambda^2}$ and the coefficients C_λ are to be determined from the boundary condition, Eq. (3). Note that the potential cannot be written in terms of the modified Bessel function K_0 because this function is not regular at $r = 0$.

By writing the step function $H(x)$ as the inverse Fourier transform of its Fourier transform [19], Eq. (3) can be rewritten as

$$\left.\frac{\partial\phi}{\partial r}\right|_{r=a}=\frac{\sigma}{2\pi\varepsilon}\int_{-\infty}^{\infty}\left[\pi\delta(\lambda)+\frac{1}{\mathrm{i}\lambda}\right]\mathrm{e}^{\mathrm{i}\lambda\kappa x}\,\mathrm{d}\lambda \tag{6}$$

where $\delta(\lambda)$ is the Dirac's delta function. Comparing Eq. (6) with the radial derivative of Eq. (5) at $r = a$

$$\left.\frac{\partial\phi}{\partial r}\right|_{r=a}=\int_{-\infty}^{\infty}C_\lambda\kappa_\lambda I_1(\kappa_\lambda a)\mathrm{e}^{\mathrm{i}\lambda\kappa x}\,\mathrm{d}\lambda \tag{7}$$

the coefficients C_λ are obtained as

$$C_\lambda=\frac{\sigma}{2\pi\varepsilon\kappa_\lambda I_1(\kappa_\lambda a)}\left[\pi\delta(\lambda)+\frac{1}{\mathrm{i}\lambda}\right] \tag{8}$$

Then, the electric potential distribution in the interfacial region is

$$\begin{aligned}\phi(r,x)&=\frac{\phi_\infty(r)}{2}+\frac{\sigma}{\varepsilon\kappa}\int_{-\infty}^{\infty}\frac{h(r,\lambda)}{2\pi\mathrm{i}\lambda}\mathrm{e}^{\mathrm{i}\lambda\kappa x}\,\mathrm{d}\lambda\\&=\frac{\phi_\infty(r)}{2}+\frac{\sigma}{\varepsilon\kappa}\int_{0}^{\infty}\frac{h(r,\lambda)}{\pi\lambda}\sin(\lambda\kappa x)\,\mathrm{d}\lambda\end{aligned} \tag{9}$$

where

$$h(r,\lambda)\equiv\frac{I_0(\kappa_\lambda r)}{\sqrt{1+\lambda^2}I_1(\kappa_\lambda a)}=h(r,-\lambda) \tag{10}$$

Since

$$\lim_{\xi\to\pm\infty}\frac{\sin(\lambda\xi)}{\pi\lambda}=\pm\delta(\lambda) \tag{11}$$

the potential ϕ tends to zero in the external bulk solution and to ϕ_∞ deep inside the charged pore, as it should be expected [19].

Fig. 2 shows the electric potential distribution in the interfacial region obtained by numerical integration of Eq. (9) for a semi-infinite pore with a fixed charge concentration $X\equiv 2\sigma/Fa=50$ mM, $\kappa a=1.0$, and a bulk electrolyte concentration $c=X$. These dimensionless parameters may correspond, for example, to $a=15$ Å, $c=50$ mM and $\sigma=0.326\ \mu\mathrm{C\,cm^{-2}}$. It can be seen that the pore entrance effects extend over a distance of the order of several Debye lengths. This smooth potential distribution should be compared to the discontinuous one assumed in the capillary charge model. In this model the electrical double layer at the membrane|solution interface is not described and the potential is assumed to jump discontinuously at $x=0$ from zero in the external side of the interface to $\phi_\infty(r)$ inside the pore. Similarly, in the classical Donnan approach for one-dimensional membrane systems, the potential is assumed to jump discontinuously at the interface from zero in the external side to $F\phi_\mathrm{D}/RT\equiv\sinh^{-1}(X/2c)$ inside the membrane. For the case $c=X$, this means $F\phi_\mathrm{D}/RT=0.481$ which obviously is intermediate between $F\phi_\infty(0)/RT=0.448$ and $F\phi_\infty(a)/RT=0.560$ because the Donnan potential in the one-dimensional approach is a kind of average potential over the cross-section.

It should be noted that $\phi(r,0)=\phi_\infty(r)/2$ at the interface. That is, in the linear approximation of the PB equation, the potential drop in the solution side of the interfacial region is equal to that in the membrane side. This is no longer true in highly charged membranes [8]. The potential distribution in the interfacial region cannot be obtained in analytical closed form, and the nonlinear Poisson–Boltzmann equation

$$\frac{1}{r}\frac{\partial}{\partial r}\left(r\frac{\partial\phi}{\partial r}\right)+\frac{\partial^2\phi}{\partial x^2}=\frac{RT\kappa^2}{F}\sinh\left(\frac{F\phi}{RT}\right) \tag{12}$$

needs then to be solved numerically. Fig. 3 shows the numerical solution obtained by using a finite element method (FEMLAB 3.0) for the case $X=0.4$ M, $c=X/8=50$ mM and $\kappa a=1.0$, which corresponds to a classical Donnan potential of $F\phi_\mathrm{D}/RT=2.09$. This potential distribution is qualitatively similar to that computed from our analytical solution in the linear approximation, Fig. 2, and the accuracy of the analytical approximation has also been confirmed using FEMLAB when the linear approximation is valid.

We consider next the electric potential distribution across a charged cylindrical pore of length L separating two identical 1:1 electrolyte solutions of concentration c (see Fig. 1b). The origin $x=0$ is now taken at the center of the pore. The boundary condition Eq. (3) must be replaced by

$$\left.\frac{\partial\phi}{\partial r}\right|_{r=a}=\begin{cases}\sigma/\varepsilon, & |x|<L/2\\ 0, & |x|>L/2\end{cases} \tag{13}$$

and can be written as [19]

$$\left.\frac{\partial\phi}{\partial r}\right|_{r=a}=\frac{\sigma}{\varepsilon}\int_{-\infty}^{\infty}\frac{\sin(\lambda\kappa L/2)}{\pi\lambda}\mathrm{e}^{\mathrm{i}\lambda\kappa x}\,\mathrm{d}\lambda \tag{14}$$

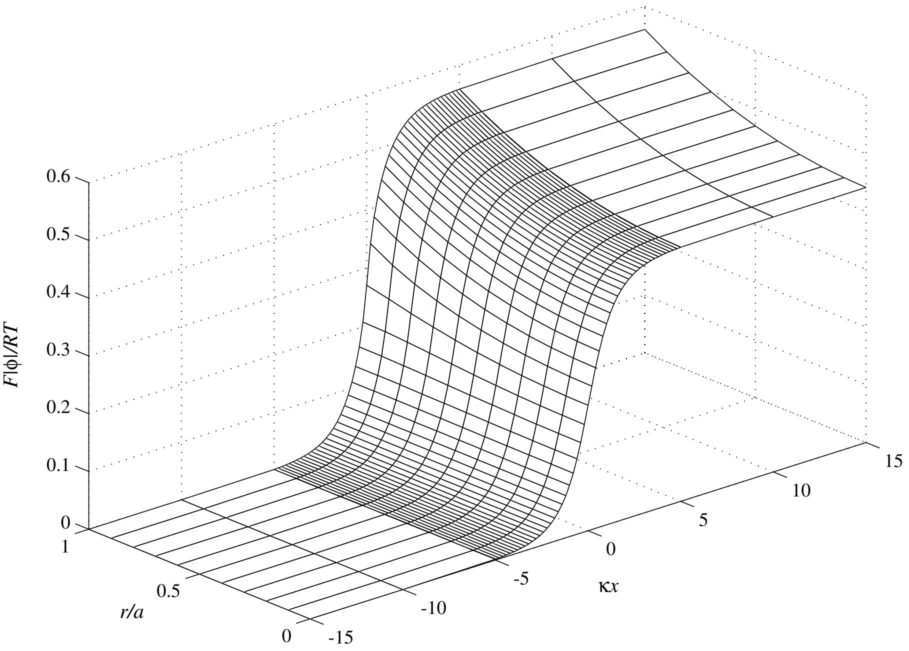

Fig. 2. Electric potential distribution (in RT/F units) for a pore with $X=50$ mM, $\kappa a=1.0$, and a bulk electrolyte concentration $c=X$.

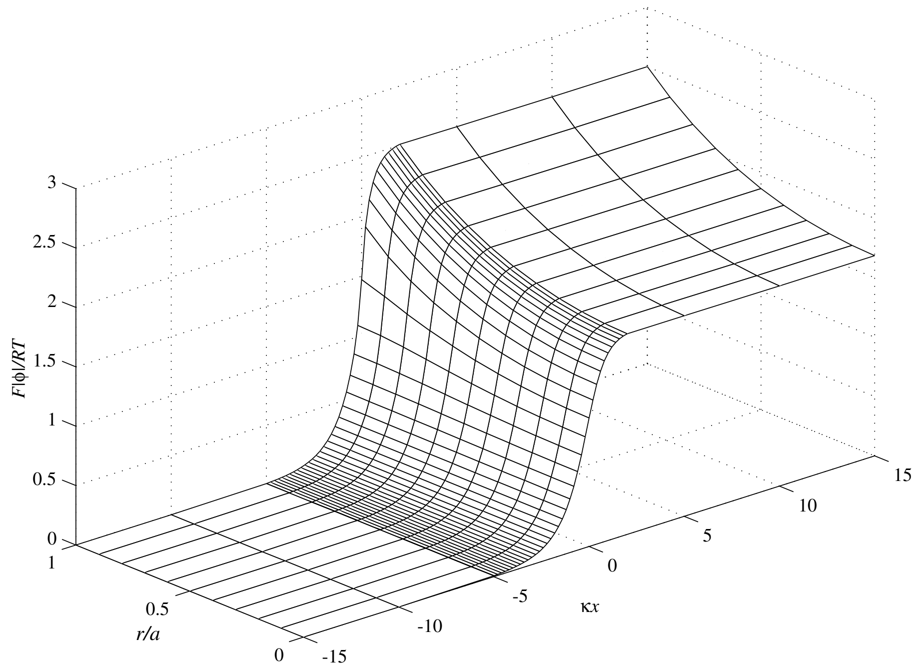

Fig. 3. Electric potential distribution (in RT/F units) for a pore with $X = 0.4$ M, $\kappa a = 1.0$, and a bulk electrolyte concentration $c = X/8 = 50$ mM. The solution has been obtained by solving Eq. (12) by means of a finite element method.

Comparing this equation with Eq. (7), the coefficients C_λ are obtained as

$$C_\lambda = \frac{\sigma}{\varepsilon\kappa_\lambda I_1(\kappa_\lambda a)} \frac{\sin(\lambda\kappa L/2)}{\pi\lambda} \tag{15}$$

and the electric potential distribution is given by Eq. (5) as

$$\begin{aligned}\phi(r,x) &= \frac{\sigma}{\varepsilon\kappa} \int_{-\infty}^{\infty} \frac{h(r,\lambda)}{\pi\lambda} \sin(\lambda\kappa L/2) \mathrm{e}^{\mathrm{i}\lambda\kappa x}\,\mathrm{d}\lambda \\ &= \frac{2\sigma}{\varepsilon\kappa} \int_{0}^{\infty} \frac{h(r,\lambda)}{\pi\lambda} \sin(\lambda\kappa L/2)\cos(\lambda\kappa x)\,\mathrm{d}\lambda \end{aligned} \tag{16}$$

where $h(r,\lambda) = h(r,-\lambda)$, is given in Eq. (10).

Fig. 4 shows the axial distribution of the electric potential across pores of different lengths and equal radii, $\kappa a = 1.0$, and fixed charge concentration $X = c = 50$ mM, as obtained by numerical integration of Eq. (16). A departure for the potential at the pore center from the value that it has for a semi-infinite pore is noticed for pores with $\kappa L < 10$.

Fig. 5 shows the electric potential distribution obtained by numerical integration of Eq. (16) for a pore of $L = 5a$, $\kappa a = 1.0$, and $X = c = 50$ mM. Again, this smooth potential distribution should be compared to that assumed in the charged capillary model, where the potential jumps discontinuously from zero at the external solution to

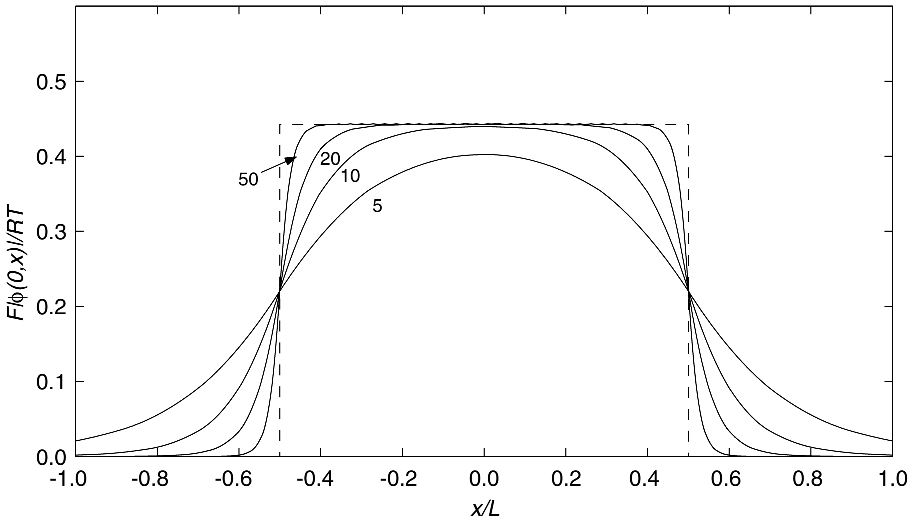

Fig. 4. Axial distribution of the electric potential across pores of different lengths (values of κL shown) and equal radii, $\kappa a = 1.0$. The rest of the parameters are the same as in Fig. 2. The curve corresponding to the discontinuous approach (dashed line) is also shown for comparison.

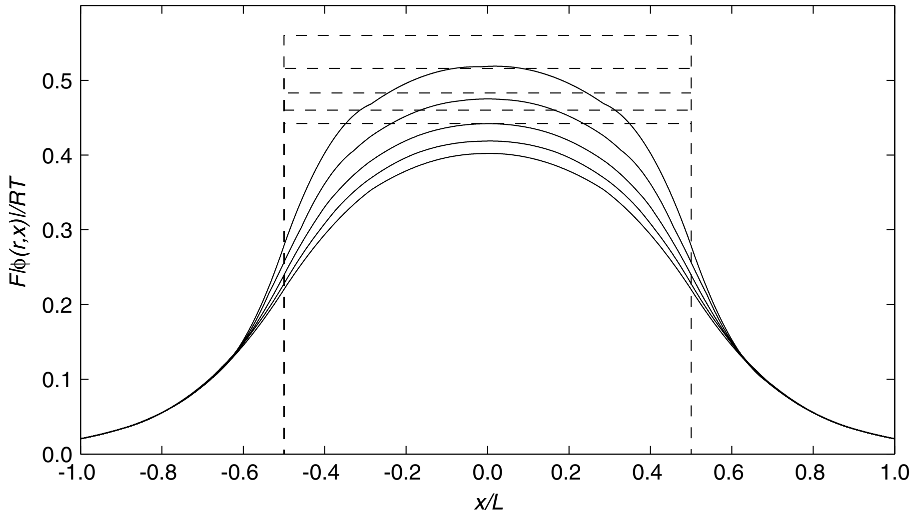

Fig. 5. Distribution of the electric potential for a pore of length $L = 5/\kappa$ and radius $a = 1.0/\kappa$ (each curve corresponds to values of r/a: 1.0, 0.8, 0.6, 0.4, 0.0 from top to bottom). The rest of the parameters are the same as in Fig. 2. Curves corresponding to the discontinuous approach (dashed lines) are also shown for comparison.

$\phi_\infty(r)$ inside the pore. The latter are shown as dashed lines in Fig. 5. It is apparent that the discontinuous formalism provides a very poor description of the axial dependence of the potential, and it also overestimates the potentials inside the pore.

Table 1 gives the ratio $\phi(0,0)/\phi_\infty(0)$ for different pore lengths. Obviously, in the limit $L \to \infty$, i.e., when the charged pore extends over the whole x axis, the potential $\phi(r,x)$ reduces to $\phi_\infty(r)$ because of Eq. (11). For the linear solution it is observed that the potential at the pore center deviates by more than 5% from ϕ_∞ when the pore length is smaller than $7/\kappa$, i.e., seven Debye lengths. This deviation is less noticeable in the nonlinear solution, which is due to the increase of both the fixed charge concentration and the concentration of mobile ions inside the pore, and leads to a more abrupt potential variation at the interface.

In this short communication we have solved analytically the linear Poisson–Boltzmann equation in the cylindrical interfacial region between a charged pore and the external solutions. The analytical solution is given in an integral form that allows us to calculate the potential distribution rather easily. This is a significant improvement over the state-of-the-art. Both, the classical one-dimensional Donnan approach and the two-dimensional capillary charged model assume discontinuous changes in the potential at the membrane|solution interface. In the latter case, this is particularly discouraging because a strong effort is made to describe the equilibrium electrical double layer in the radial direction and then the electrical double layer in the axial direction is disregarded. This is justified because edge effects are negligible when the pore length is much larger than the pore radius. However, it is also true that the capillary charge model is sometimes applied to short pores and that an analytical solution that describes the complete axial–radial distribution was not previously available. In a preliminary attempt to analyze the importance of edge effects in short pores, we have also studied the potential distribution in finite-length pores. Significant deviations from the predictions of the discontinuous formalism occur for less than ca. 10 Debye lengths for low surface charge densities (low surface potentials). We believe that the analytical solution obtained here can be useful in ion transport studies through synthetic membranes and biological ion channels.

Table 1
Ratio of the potential at the pore center to that calculated for an infinitely long pore, $\phi_\infty(0)$ for different pore lengths and the same parameters as in Figs. 2 and 3 for the linear and nonlinear solutions, respectively

κL	$\phi(0,0)/\phi_\infty(0)$	$\phi(0,0)/\phi_\infty(0)$ (nonlinear)
20	1.000	1.000
15	1.000	1.000
7.5	0.980	1.000
5.0	0.921	1.000
3.0	0.767	0.945
1.5	0.492	0.752

References

[1] N. Lakshminarayanaiah, Equations of Membrane Biophysics, Academic Press, New York, 1984.
[2] S. Levine, J.R. Marriott, G. Neale, N. Epstein, J. Colloid Interface Sci. 52 (1975) 136.
[3] P.N. Pintauro, M.W. Verbrugge, J. Membrane Sci. 44 (1989) 197.
[4] S. Basu, M. Sharma, J. Membrane Sci. 124 (1997) 77.
[5] A.G. Guzmán-Garcia, P.N. Pintauro, M.W. Verbrugge, R.F. Hill, AIChE J. 36 (1990) 1061.
[6] R. Schlögl, Ph.D. thesis, Georg August University of Göttingen, 1953.
[7] H. Ohshima, S. Ohki, Biophys. J. 47 (1985) 673.
[8] I.C. Bassignana, H. Reiss, J. Phys. Chem. 87 (1993) 136–149.
[9] J.A. Manzanares, S. Mafé, J. Bisquert, Ber. Bunsenges. Phys. Chem. 96 (1992) 538.
[10] A.D. MacGillivray, J. Chem. Phys. 48 (1968) 2903.

[11] F. Helfferich, Ion Exchange, McGraw Hill, New York, 1962.
[12] T.S. Sørensen (Ed.), Surface Chemistry and Electrochemistry of Membranes, Surfactant Science Series, vol. 79, Marcel Dekker, New York, 1999 (Chapters 17–20 and 22–23).
[13] B. Hille, Ionic Channels of Excitable Membranes, Sinauer, Sunderland, 2001.
[14] T.S. Sørensen, J. Koefoed, J. Chem. Soc. Faraday Trans. II 70 (1974) 665.
[15] S. Mafé, J.A. Manzanares, J. Pellicer, J. Membrane Sci. 51 (1990) 161.
[16] L. Martínez, A. Hernández, A. González, F. Tejerina, J. Colloid Interface Sci. 152 (1992) 325.
[17] V.M. Aguilella, M. Aguilella-Arzo, P. Ramírez, J. Membrane Sci. 113 (1996) 191.
[18] J. Cervera, J.A. Manzanares, S. Mafé, J. Membrane Sci. 191 (2001) 179.
[19] K.F. Riley, M.P. Hobson, S.J. Bence, Mathematical Methods for Physics and Engineering, Cambridge U.P., Cambridge, 2002, (Chapters 12 and 19).